Ž.Kovačević[1], R.Hayn[2], N.M.Plakida

EFFECTIVE HUBBARD MODEL
FOR Zn-DOPED CuO$_2$ PLANE

[1]Faculty of Natural Science and Mathematics, University of Montenegro,
P.O.Box 211, 81001 Podgorica, Yugoslavia
[2]Institute for Theoretical Physics, University of Technology Dresden,
D-01062 Dresden, Germany

1 Introduction

In order to test different theories for the electronic structure and a mechanism of high-temperature superconductivity in cuprates, many experimental studies of impurity effects have been made (see, e.g., [1]). In comparing with other trivalent and divalent, magnetic and nonmagnetic dopants, a striking peculiarity induced by the substitution of nonmagnetic Zn ions with $3d^{10}$ closed shell into the Cu site has attracted much attention. The most unexpected result is a strong deterious effect on superconductivity without changing carrier concentration in low Zn-doped samples (see, e.g., [2]). At the same time an appreciable reduction of the Néel temperature T_N by Zn substitution was observed both in $La_2Cu_{1-y}Zn_yO_4$ [3] and $YBa_2(Cu_{1-y}Zn_y)_3O_{6+x}$ [4] compounds. In $La_2Cu_{1-y}Zn_yO_4$ compound $T_N \rightarrow 0$ at Zn concentration of $y \simeq 0.055$ [3] that is much smaller than the site percolation threshold of 0.41 for a square lattice. With doping the reduction of the Néel temperature by Zn impurities increases [4].

The formation of the induced magnetic moment by Zn substitution in cuprates was found out in several studies. Measurement of the static magnetic susceptibility revealed the Curie law with static magnetic moment of the order $1\mu_B$ per Zn-site for the underdoped region which decreased with Sr doping in $La_{2-x}Sr_xCu_{1-y}Zn_yO_4$ [3, 5]. NMR experiments in $YBa_2(Cu_{1-y}Zn_y)_3O_{6+x}$ [4, 6] have revealed that induced local magnetic moments resides on the nearest neighbour Cu orbitals. The local magnetic moments induced by Zn doping were also observed in electron paramagnetic resonance [7] and μSR [8] experiments. The local magnetic moments can be induced also by other nonmagnetic substitutions with closed shells like Al^{3+} and Ga^{3+} [5, 9].

In NMR and NQR measurements [10] the authors observed a local suppression of antiferromagnetic spin correlations near Zn impurities and an induced
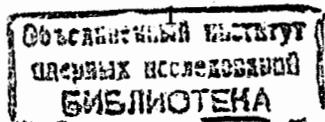
finite density of states at the Fermi level. Further investigations by Gd^{3+} ESR [11] and by NMR [12] have confirmed that in the regions around Zn ions both the superconducting and spin excitation gaps are suppressed as it has been observed earlier in the electronic specific heat measurements [13].

A more detailed picture of the evolution of the spin-fluctuation spectra induced by Zn substitution in $YBa_2(Cu_{1-y}Zn_y)_3O_{6+x}$ was obtained by inelastic neutron scattering. In the underdoped sample with $x = 0.6$ the quasi-gap behaviour in spin fluctuations at the antiferromagnetic wave vector (π, π) in the pure, superconducting sample disappears upon Zn doping [14]. In the overdoped compound with $x = 0.97$ the spin-fluctuation spectrum below T_c changes drastically [15]. In the zinc-free sample it has a gap below 35 meV and a resonance region around 41 meV. In the sample with Zn concentration $y = 0.02$ the gap is closed and a broad spectrum in a low energy range appears with a much lower intensity in the resonance region.

A large increase of residual resistivity induced by Zn impurities has been detected in [16]-[18]. In the underdoped regime only a few percent of Zn results in the residual resistivity close to the universal two-dimensional resistance for a potential scatterer in the unitary limit, $h/4e^2$. At this universal value of the sheet resistance for various combinations of doped hole and Zn concentrations a transition from superconducting to insulating state occurs. In the highly doped regime the universal behaviour was not seen.

These experiments have proved that the Zn^{+2} ion cannot be considered just as an inert substitution in the CuO_2 plane in spite of its nonmagnetic state with the $3d$ closed shell. It reveals itself as a strong potential scattering centre which also suppresses antiferromagnetic spin correlations at the nearest Cu sites. These properties of Zn impurity should be responsible for the strong reduction of superconducting T_c for the d-wave pairing. As estimations show [19, 9],

the pair-breaking effect due to induced magnetic moments gives an order of magnitude smaller contribution in comparison with the experimental results.

Several theoretical models have been proposed to explain the anomalous behaviour of Zn impurity in copper oxides [20]-[32]. In a number of papers the Zn impurity in the CuO_2 plane was considered as a local nonmagnetic impurity level at high energy in the Hubbard model [21, 22] or the t-J model [23]. Using the T-matrix description, bound impurity states within the Hubbard gap were obtained. Due to strong Coulomb correlations in the model, the bare local impurity potential becomes a dynamic one that results in the resonant scattering and bound state formation of different (p, d-wave) symmetries in the gap. Formation of local magnetic moments induced by a spin vacancy within the RVB theory in the two-dimensional spin liquid in the underdoped cuprates was considered in [7, 24, 25]. Influence of the impurity local moments on magnetic and transport properties in the RVB state were studied within the slave-boson and slave-fermion mean-field theories in [26]. The importance of $4s$ orbital for Zn^{2+} impurity in charge transfer excitations between copper $3d$ and zinc $4s$ orbitals was pointed out in [27]. To investigate the influence of nonmagnetic impurities on the d-wave superconductivity several phenomenological models of Fermi liquid type have been also considered (see, e.g., [28]-[32]).

However, to justify the proposed simple models a microscopical theory of electronic spectrum for the CuO_2 plane with a proper consideration of both the strongly correlated $3d$ states on copper and zinc sites and $2p$ states on oxygen sites should be developed. In the present paper we propose a microscopical approach based on the original p-d model [33, 34] and derive an effective Hubbard model describing a low-energy electronic spectrum of the Zn-doped CuO_2-plane. Based on the band structure calculations for a model $CaCuO_2$ compound with Zn substitution in Sec. 2, we conclude that Zn $3d^{10}$ orbitals

can be neglected in comparison with Cu $3d$-orbitals and O $2p$-orbitals. So starting from the three-band p-d Hubbard model with Zn sites considered as a vacant Cu-site and employing the cell-perturbation method [35]-[39] we derive in Sec.3 an effective Hubbard model. In the model the host lattice has one-hole states of a predominantly Cu $3d$-like character and two-hole Zhang-Rice singlet Cu-O states [40] while at the impurity Zn sites the lowest levels are the one-hole Wannier oxygen doublet states. Further reduction to an effective $t - J$ model in Sec. 4 reveals a large ferromagnetic superexchange interaction between the Cu spin with the nearest virtual oxygen spin in the Zn cell. Conclusions are presented in Sec. 5.

2 Band structure of Zn-doped CaCuO$_2$ compound

To obtain a first information about the effect of zinc impurities in cuprates we performed band-structure calculations. We have chosen as the basis of our investigation one of the simplest undoped cuprates containing CuO$_2$ planes, namely CaCuO$_2$. It is an idealised parent compound to the simple tetragonal Ca$_{0.86}$Sr$_{0.14}$CuO$_2$ where the Sr $\rightarrow$ Ca substitution is necessary to stabilise the tetragonal phase but is electronically unimportant. That compound was also chosen in Ref. [41] as an ideal model system to investigate the electronic structure due to its structural simplicity. It has the space group $P4/mmm$ and lattice parameters $a = 3.86$ Å and $c = 3.20$ Å. It consists of CuO$_2$ planes which are separated by Ca layers and is more three-dimensional than, say La$_2$CuO$_4$. To investigate the effect of zinc impurities we replaced each second copper atom by zinc in a chess-board-like pattern and calculated also the band-structure of the hypothetical compound Ca$_2$CuZnO$_4$ having a twice as large unit cell.

The calculations were done in the local density approximation (LDA)

using the linear combination of atomic orbitals (LCAO). Due to the relatively open structure one or two empty spheres per unit cell for CaCuO$_2$ or Ca$_2$CuZnO$_4$, respectively, have been introduced (in the Ca plane). The calculation was scalar relativistic and we have chosen a minimal basis set consisting of Cu($4s,4p,3d$), Zn($4s,4p,3d$), O($2s,2p$) and Ca($4s,4p,3d$) orbitals. The lower-lying states were treated as core states. To optimise the local basis a contraction potential has been used at each site [42]. The exchange and correlation part was treated in the atomic sphere approximation, while the Coulomb part of the potential was constructed as a sum of overlapping spherical contributions.

The resulting density of states (DOS) for CaCuO$_2$ is shown in Fig. 1. The dispersion of the bands in the Brillouin zone is not shown but it coincides nearly with the result given in Ref. [41]. In contrast with the expected insulating behaviour of an undoped cuprate we obtain a metallic state due to the neglect of strong electron correlations in the LDA. The Fermi level lies in the antibonding copper $3d$ – oxygen $2p$ band. The main effect of the electron correlation is to split that band into two Hubbard subbands that results in a gap opening of roughly 2 eV . In the further discussion of the LDA results we will assume that the other effects of electron correlations on the electronic structure of the valence band are less important. We show also the partial Cu- and O-DOS in Fig. 1 which indicate already the strong hybridisation between Cu $3d$ and O $2p$ orbitals throughout the whole valence band. There is a small contribution of Cu $4s$ and O $2s$ orbitals at the Fermi level: we had to multiply the corresponding DOS by a factor of 10 to be visible.

Let us now compare the DOS for Ca$_2$CuZnO$_4$ (Fig. 2) with the reference DOS of CaCuO$_2$ (Fig. 1). First of all, we observe *all* the Zn $3d$ states deep below the Fermi level at around 8 eV binding energy. That confirms the simple
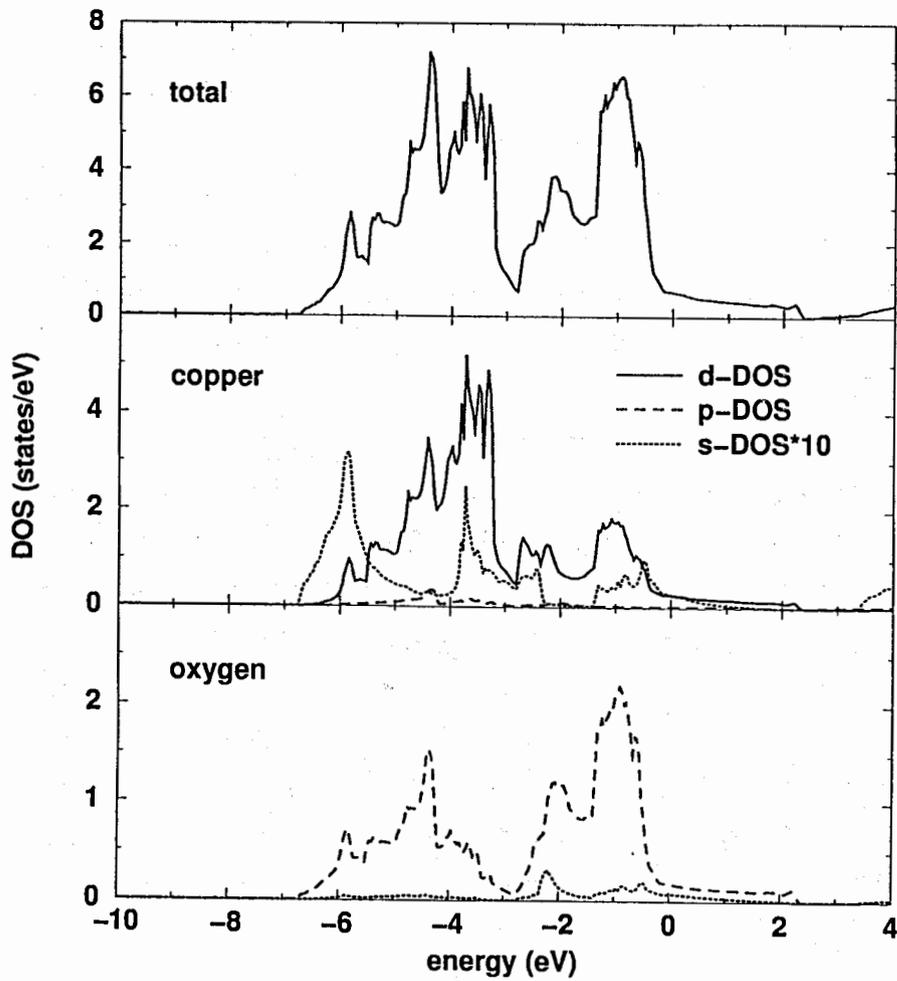
Figure 1: Total and partial densities of states for CaCuO$_2$. The Fermi level corresponds to the zero of energy.
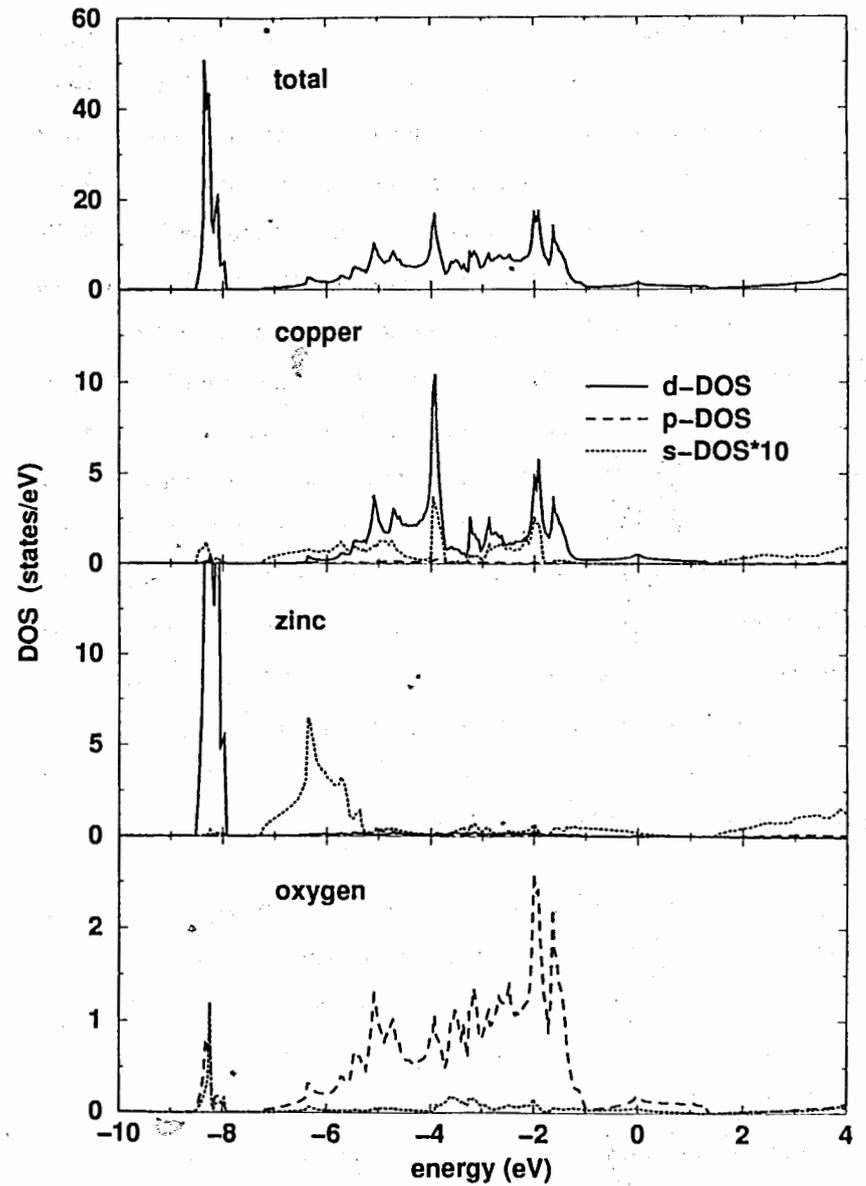
Figure 2: Total and partial densities of states for Ca$_2$CuZnO$_4$. The Fermi level is at zero energy.

chemical argument that there should be one hole in the d shell of copper (configuration d^9) but no hole in the d shell of zinc (d^{10}) (which neglects, however, the d-p hybridisation between copper and oxygen). Besides that difference concerning the zinc d levels there is some similarity in the valence band structures of $CaCuO_2$ and Ca_2CuZnO_4. The main band consisting of Cu $3d$ and O $2p$ states has a bandwidth of about 9 eV in both cases. More detailed analysis shows that the band crossing Fermi level is built of the Cu $3d_{x^2-y^2}$ and in-plane oxygen $2p$ orbitals. But its bandwidth is smaller for Ca_2CuZnO_4 due to less copper neighbours at an oxygen site. One can expect that for a small zinc concentration the original bandwidth should be recovered. But the position of the zinc $3d$ levels at around 8 eV should be stable for different amounts of zinc impurities. There is nearly no Cu $4s$ DOS at the Fermi level in Fig. 2 but some Zn $4s$ DOS. Due to its smallness we neglect the $4s$ states in the construction of the model Hamiltonian in the following section. Its inclusion will only be necessary for a more refined picture.

3 Derivation of effective Hubbard model

According to the results of band structure calculations presented in Sec. 2 we neglect the Zn orbitals in a tight binding modelling of Zn-doped CuO_2 plane with the main effect of Zn doping being a creation of vacant Cu-sites. At the same time we suggest that the energy levels of O-$2p$ orbitals are not considerably changed by substitution of Zn^{2+} for Cu^{2+}. Therefore, in a conventional tight binding description of the CuO_2 plane with copper $3d_{x^2-y^2}$ and oxygen $2p_x$ and $2p_y$ hole σ-orbitals, one can model Zn-impurities by vacant $3d_{x^2-y^2}$ sites. Taking into account only the most important terms, in the limit of strong correlations at the Cu-site ($U_d \to \infty$), we consider the following p-d model Hamiltonian [33, 34]

$$H = \epsilon_d \sum_{i\sigma} \hat{d}^+_{i\sigma}\hat{d}_{i\sigma} + \epsilon_p \sum_{m\sigma} p^+_{m\sigma}p_{m\sigma} + \sum_{im\sigma}(t^{pd}_{im}\hat{d}^+_{i\sigma}p_{m\sigma} + \text{H.c.}) + \sum_{mn\sigma}(t^{pp}_{mn}p^+_{m\sigma}p_{n\sigma} + \text{H.c.}),$$

(1)

where i-sites contain only Cu (i.e. $i \ni Cu$) and m, n sites contain O atoms (i.e. $m, n \ni O$) while the the sum over Zn-sites, being vacant for the Cu sublattice, is omitted. Here ϵ_d and $\epsilon_p = \epsilon_d - \Delta_{pd}$ are the energies of the localised holes on Cu and O sites, respectively. The sign of the hopping integrals $t^{pd}_{im} = t_{pd}\text{sgn}(S_{im})$ and $t^{pp}_{mn} = t_{pp}\text{sgn}(S_{mn})$ are chosen according to the sign-convention for the coefficients S_{im}, S_{mn} used in [39]. The fitting parameters of the model are the difference between the energy levels, $\Delta_{pd} = \epsilon_p - \epsilon_d \simeq 4$ eV, and the hopping integrals, $t_{pd} \simeq 1.5$ eV and $t_{pp} \simeq 0.6$ eV (see, e.g., [36]-[38]). We used the hole representation in Eq.(1) with the vacuum state $|3d^{10}2p^6 >$ for both the Cu and Zn sites where $\hat{d}^+_{i\sigma} = d^+_{i\sigma}(1 - n_{i\bar\sigma})$ operators create a hole on a copper site i providing that there is no other hole with the spin $\bar\sigma = -\sigma$ and the operators $p^+_{m\sigma}$ create a hole with the spin σ on the oxygen sites m, $\sigma = \pm 1$.

Using unitary transformation from the Fourier component of the original canonical Fermi operators $\{p^{(x)}_{q\sigma}, p^{(y)}_{q\sigma}\}$ to the canonical Fermi operators $\{b_{q\sigma}, a_{q\sigma}\}$ [43, 36, 44]

$$\begin{pmatrix} b_{q\sigma} \\ a_{q\sigma} \end{pmatrix} = S \begin{pmatrix} p^{(x)}_{q\sigma} \\ p^{(y)}_{q\sigma} \end{pmatrix},$$

(2)

with [39]

$$S = \frac{i}{\lambda_q} \begin{pmatrix} S_{qx} & -S_{qy} \\ S_{qy} & S_{qx} \end{pmatrix},$$

(3)

where $\lambda^2_q = S^2_{qx} + S^2_{qy}$, $S_{q\alpha} = \sin(q_\alpha/2)$, $\alpha = (x, y)$, one derives

$$H = \epsilon_d \sum_{i\sigma} \hat{d}^+_{i\sigma}\hat{d}_{i\sigma} + \epsilon_p \sum_{j\sigma}(b^+_{j\sigma}b_{j\sigma} + a^+_{j\sigma}a_{j\sigma}) + 2t_{pd}\sum_{ij\sigma}\{\lambda(i-j)\hat{d}^+_{i\sigma}b_{j\sigma} + \text{H.c.}\}$$
$$- t_{pp}\sum_{kj\sigma}\{\mu(k-j)(b^+_{k\sigma}b_{j\sigma} - a^+_{k\sigma}a_{j\sigma}) - \nu(k-j)(a^+_{k\sigma}b_{j\sigma} + b^+_{k\sigma}a_{j\sigma})\}.$$

(4)

Coefficients of the oxygen Wannièr orbitals (5). $\mathbf{R}(i-j)$ is the radius vector connecting cell sites i and j, $\hat{x}$ and $\hat{y}$ are the basis cell vectors. Only the coefficient ν has sign-changing symmetry: $\nu(x,y) = -\nu(y \cdot \mathrm{sgn}x, x \cdot \mathrm{sgn}y)$ [37, 39].

$\mathbf{R}$(i-j)	λ	μ	ν
$\mathbf{0}$	0.958	1.454	0.0
$\hat{x}$	-0.140	-0.546	-0.266
$\hat{x}+\hat{y}$	-0.023	0.244	0.0
$2\hat{x}$	-0.014	-0.128	0.082

Here the operators $b_{j\sigma}^+ (a_{j\sigma}^+)$ acting on the vacuum create holes with the spin σ on the orthogonalised oxygen Wannièr orbitals associated with the cells $i \ni$ Cu and $j,k \ni$ Cu or Zn.

The corresponding Wannièr coefficient is given by

$$\{\lambda,\mu,\nu\}(i-j) = \frac{1}{N}\sum_{\mathbf{q}}\{\lambda,\mu,\nu\}_{\mathbf{q}}e^{i\mathbf{q}(\mathbf{R_i}-\mathbf{R_j})}, \qquad (5)$$

where $\mu_{\mathbf{q}} = 8S_{qx}^2 S_{qy}^2/\lambda_q^2$ and $\nu_{\mathbf{q}} = 4S_{qx}S_{qy}(S_{qx}^2 - S_{qy}^2)/\lambda_q^2$.

The summation over $\mathbf{q}$ is made inside the first Brillouin zone and the coefficients λ,μ,ν decrease rapidly with the distance $|\mathbf{R}_i - \mathbf{R}_j|$ between the cell sites i and j, as can be seen from the Table 1.

In the framework of the cell-perturbation method [35]-[39], it is useful to divide the Hamiltonian into the intracell and intercell parts as follows

$$H = H_{loc} + H_{hop}, \qquad (6)$$

where

$$H_{loc} = \epsilon_d \sum_{i\sigma} \hat{d}_{i\sigma}^+ \hat{d}_{i\sigma} + \sum_{j\sigma}(\epsilon_p^{(-)} b_{j\sigma}^+ b_{j\sigma} + \epsilon_p^{(+)} a_{j\sigma}^+ a_{j\sigma}) + \sum_{i\sigma}(V_0^{pd}\hat{d}_{i\sigma}^+ b_{i\sigma} + \text{H.c.}), \quad (7)$$

where $i \ni$ Cu and $j \ni$ Cu or Zn, $V_0^{pd} = 2t_{pd}\lambda_0$ and $\epsilon_p^{(\pm)} = \epsilon_p \pm \mu_0 t_{pp}$.

$$H_{hop} = \sum_{i \ne j,\sigma}\{V_{ij}^{pd}\hat{d}_{i\sigma}^+ b_{j\sigma}+\text{H.c}\} - \sum_{j \ne k,\sigma}\{V_{jk}^{pp}(b_{j\sigma}b_{k\sigma}-a_{j\sigma}^+ a_{k\sigma})-W_{jk}^{pp}(a_{j\sigma}^+ b_{k\sigma}+b_{j\sigma}^+ a_{k\sigma})\}, \qquad (8)$$

where $i \ni$ Cu cells and $k,j \ni$ Cu or Zn cells and

$$V_{ij}^{pd} = 2t_{pd}\,\lambda(i-j), \quad V_{ij}^{pp} = t_{pp}\,\mu(i-j), \quad W_{ij}^{pp} = t_{pp}\,\nu(i-j). \qquad (9)$$

Exact diagonalisation of the intracell part H_{loc}, for the cells containing Cu, gives the lowest one-hole, predominantly d-type state

$$|D\sigma> = \cos\theta_1 d_\sigma^+|0> - \sin\theta_1 b_\sigma^+|0>,$$

with the corresponding energy

$$E_D = \frac{1}{2}(\epsilon_p^{(-)} + \epsilon_d) - \frac{1}{2}\sqrt{(\epsilon_p^{(-)} - \epsilon_d)^2 + 4(V_0^{pd})^2}. \qquad (10)$$

The lowest two-hole state which can be identified as the generalised Zhang-Rice singlet [40] is given by

$$|\psi> = \cos\theta_2 \frac{1}{\sqrt{2}}(d_\uparrow^+ b_\downarrow^+ - d_\downarrow^+ b_\uparrow^+)|0> - \sin\theta_2 b_\uparrow^+ b_\downarrow^+|0>,$$

with the corresponding energy

$$E_\psi = \frac{1}{2}(3\epsilon_p^{(-)} + \epsilon_d) - \frac{1}{2}\sqrt{(\epsilon_p^{(-)} - \epsilon_d)^2 + 8(V_0^{pd})^2}, \qquad (11)$$

where

$$\cos\theta_1 = \sqrt{\frac{1}{2}\{1 + \frac{\epsilon_p^{(-)} - \epsilon_d}{\sqrt{(\epsilon_p^{(-)} - \epsilon_d)^2 + 4(V_0^{pd})^2}}\}}, \qquad (12)$$

$$\cos\theta_2 = \sqrt{\frac{1}{2}\{1 + \frac{\epsilon_p^{(-)} - \epsilon_d}{\sqrt{(\epsilon_p^{(-)} - \epsilon_d)^2 + 8(V_0^{pd})^2}}\}}. \qquad (13)$$

For cells containing Zn, the lowest one-hole doublet states $|b\sigma> = b_\sigma^+|0>$ has the energy $\epsilon_p^{(-)} = \epsilon_p - \mu_0 t_{pp}$.

Reduction to an effective two-band model is achieved by reducing the size of the Hilbert subspace to the lowest states in the one-hole and two-hole sectors [36]-[38], [44], leaving only one-hole doublet states $|b\sigma>$ for impurity cells. By introducing the projection Hubbard operators $X_i^{\alpha,\beta} \equiv (|\alpha>)_i(<\beta|)_i$ for the quantum states $|\alpha>, |\beta>$ in the cell i we obtain

$$H_{loc} \simeq E_D \sum_{i\sigma} X_i^{D\sigma,D\sigma} + E_\psi \sum_i X_i^{\psi,\psi} + \epsilon_p^{(-)} \sum_{k\sigma} X_k^{b\sigma,b\sigma}, \qquad (14)$$

$$H_{hop}^{Cu-Cu} \simeq \sum_{i\neq j,\sigma} \{t_{ij}^{\psi\psi} X_i^{\psi,D\sigma} X_j^{D\sigma,\psi} + t_{ij}^{DD} X_i^{D\sigma,0} X_j^{0,D\sigma} + \sigma t_{ij}^{\psi D}(X_i^{D\sigma,0} X_j^{D\bar\sigma,\psi} + \text{H.c.})\}, \qquad (15)$$

$$H_{hop}^{Cu-Zn} \simeq \sum_{i\neq k,\sigma} \{t_{ik}^{\psi b}\sigma(X_i^{\psi,D\bar\sigma} X_k^{0,b\sigma} + \text{H.c.}) + t_{ik}^{Db}(X_i^{D\sigma,0} X_k^{0,b\sigma} + \text{H.c.})\}, \qquad (16)$$

where now and what follows we use the indices (i,j) for the cells with Cu $(i, j \ni \text{Cu})$ and the index (k) only for the impurity cells with Zn $(k \ni \text{Zn})$. The effective hopping parameters between the cells containing Zn and Cu are given by

$$t_{ij}^{\psi\psi} = K_{\psi\psi} V_{ij}^{pd} - A_c^2 \cdot V_{ij}^{pp}, \quad t_{ij}^{DD} = K_{DD} V_{ij}^{pd} - V_{ij}^{pp} \sin^2\theta_1,$$

$$t_{ij}^{\psi D} = K_{\psi D} V_{ij}^{pd} + A_c V_{ij}^{pp} \sin\theta_1, \quad t_{ik}^{\psi b} = A_d V_{ik}^{pd} - A_c V_{ik}^{pp}, \qquad (17)$$

$$t_{ik}^{Db} = V_{ik}^{pd} \cos\theta_1 + V_{ik}^{pp} \sin\theta_1,$$

where

$$K_{\psi\psi} = 2A_d A_c, \quad K_{DD} = -2\sin\theta_1\cos\theta_1, \quad K_{\psi D} = A_c\cos\theta_1 - A_d\sin\theta_1$$

with the corresponding coefficients

$$A_d = -\frac{1}{\sqrt{2}}\sin\theta_1\cos\theta_2, \quad A_c = \sin\theta_1\sin\theta_2 + \frac{1}{\sqrt{2}}\cos\theta_1\cos\theta_2.$$

In this way, we obtain a two-band Hubbard-like model with one-hole Wannier oxygen levels in the Zn-cells. By neglecting H_{hop}^{Zn-Zn} term in the limit of low Zn-impurity concentration, we can write the effective two-band Hubbard model for CuO$_2$ plane with Zn impurities in the final form:

$$H \simeq H_{loc} + H_{hop}^{Cu-Cu} + H_{hop}^{Cu-Zn} - \mu N, \qquad (18)$$

where μ is the chemical potential and

$$N = \sum_i (2X_i^{\psi,\psi} + \sum_\sigma X_i^{D\sigma,D\sigma}) + \sum_{k\sigma} X_k^{b\sigma,b\sigma} \qquad (19)$$

is the number operator for which $[N, H] = 0$ is satisfied.

4 Reduction to extended t-J model

In order to compare the corresponding t-J model for a pure CuO$_2$ plane [40] and for a Zn-doped one we further reduce the two-band model (18) to the one-band one. To separate terms describing motions inside and between singlet and one-particle bands, it is convenient to rearrange the Hamiltonian (18) in the following way

$$H = H_0 + H_1 + H_1' \qquad (20)$$

$$H_0 = H_{loc} - \mu N, \quad H_1 = T_{11} + T_{22}, \quad H_1' = (T_{12} + T_{\bar12} + T_{1\bar1}) + \text{H.c.},$$

where

$$T_{11} = \sum_{i\neq j,\sigma} t_{ij}^{DD} X_i^{D\sigma,0} X_j^{0,D\sigma}, \quad T_{22} = \sum_{i\neq j,\sigma} t_{ij}^{\psi\psi} X_i^{\psi,D\sigma} X_j^{D\sigma,\psi},$$

$$T_{12} = \sum_{i\neq j,\sigma} \sigma t_{ij}^{\psi D} X_i^{D\sigma,0} X_j^{D\bar\sigma,\psi}, \quad T_{\bar12} = \sum_{i\neq k,\sigma} \sigma t_{ik}^{\psi b} X_k^{b\sigma,0} X_i^{D\bar\sigma,\psi}, \qquad (21)$$

$$T_{1\bar1} = \sum_{i\neq k,\sigma} t_{ik}^{Db} X_i^{D\sigma,0} X_k^{0,b\sigma},$$

where $i, j \ni$ Cu cells and $k \ni$ Zn cells.

Using the Schrieffer-Wolff transformation [45]

$$\tilde H = e^S H e^{-S} \simeq H_0 + H_1 + [S, H_1] + \frac{1}{2}[S, H_1'], \qquad (22)$$

one can obtain an effective Hamiltonian $\tilde{H}$ without interband hopping H_1'. The generator of the transformation S determined by the condition $H_1' + [S, H_0] = 0$ is given by

$$S = (A \cdot T_{12} + B \cdot T_{\bar{1}2} + C \cdot T_{1\bar{1}}) - \text{H.c.}, \tag{23}$$

where the coefficients are

$$A = \frac{1}{2E_D - E_\psi}, \quad B = \frac{1}{E_D - E_\psi + \epsilon_p^{(-)}}, \quad C = \frac{1}{E_D - \epsilon_p^{(-)}}. \tag{24}$$

Performing the commutations in (22), one obtains

$$\tilde{H} = H_0 + H_1 + \frac{1}{2}[S, H_1']_{2x} + \tilde{H}_{sx}, \tag{25}$$

where

$$\frac{1}{2}[S, H_1']_{2x} = -A \cdot \sum_{i \neq j,\sigma} (t_{ij}^{\psi D})^2 \{ X_i^{D\sigma, D\sigma} X_j^{D\bar{\sigma}, D\sigma} - X_i^{D\sigma, D\sigma} X_j^{D\bar{\sigma}, D\bar{\sigma}}$$

$$+ X_i^{\psi, 0} X_j^{0,\psi} + X_i^{\psi, \psi} X_j^{0,0} \}$$

$$-B \cdot \sum_{i \neq k,\sigma} (t_{ik}^{\psi b})^2 \{ X_i^{D\sigma, D\sigma} X_k^{b\bar{\sigma}, b\sigma} - X_i^{D\sigma, D\sigma} X_k^{b\bar{\sigma}, b\bar{\sigma}} + X_i^{\psi, \psi} X_k^{0,0} \}$$

$$-C \cdot \sum_{i \neq k,\sigma} (t_{ik}^{Db})^2 \{ X_i^{0,0} X_k^{b\sigma, b\sigma} - X_i^{D\sigma, D\sigma} X_k^{0,0} \}, \tag{26}$$

where $i, j \ni$ Cu cells and $k \ni$ Zn cells. The remaining part $\tilde{H}_{sx}$ with products of three Hubbard X-operators at different lattice sites

$$\tilde{H}_{sx} = [S, H_1]_{sx} + \frac{1}{2}[S, H_1']_{sx} \tag{27}$$

is given in the Appendix.

Now we introduce spin operators for Cu-sites

$$S_i^z = \frac{1}{2}\sum_\sigma \sigma X_i^{D\sigma, D\sigma}, \quad S_i^\sigma = X_i^{D\sigma, D\bar{\sigma}}, \tag{28}$$

and a spin operator for the oxygen orbital $|b\sigma>$ at Zn cell

$$s_k^z = \frac{1}{2}\sum_\sigma \sigma X_k^{b\sigma, b\sigma}, \quad s_k^\sigma = X_k^{b\sigma, b\bar{\sigma}}, \tag{29}$$

14

with $\sigma = \pm 1$. Then we obtain the effective Hamiltonian in the form of the corresponding t-J model for Zn-doped CuO_2-plane

$$\tilde{H} = \tilde{H}_0 + \tilde{H}_t + \tilde{H}_J + \tilde{H}_{sx} + \Delta\tilde{H}, \tag{30}$$

$$\tilde{H}_0 = \sum_{i\sigma} \tilde{E}_D(i) X_i^{D\sigma, D\sigma} + \sum_{k\sigma} \tilde{\epsilon}_p^{(-)}(k) X_k^{b\sigma, b\sigma} + \sum_i \tilde{E}_\psi(i) X_i^{\psi, \psi}, \tag{31}$$

$$\tilde{H}_t = \sum_{i \neq j,\sigma} t_{ij}^{DD} X_i^{D\sigma, 0} X_j^{0, D\sigma} + \sum_{i \neq j,\sigma} t_{ij}^{\psi\psi} X_i^{\psi, D\sigma} X_j^{D\sigma, \psi}, \tag{32}$$

$$\tilde{H}_J = \sum_{i \neq j} J_{ij}^{DD} (\mathbf{S}_i \cdot \mathbf{S}_j - \frac{1}{4} N_i N_j) + \sum_{i \neq k} J_{ik}^{Db} (\mathbf{S}_i \cdot \mathbf{s}_k - \frac{1}{4} N_i n_k), \tag{33}$$

$$\Delta\tilde{H} = -2A \sum_{i \neq j} (t_{ij}^{\psi D})^2 X_i^{\psi, 0} X_j^{0, \psi} + \sum_{i \neq k,\sigma} \{ B (t_{ik}^{\psi b})^2 + C (t_{ik}^{Db})^2 \} X_i^{\psi, \psi} X_k^{b\sigma, b\sigma} \tag{34}$$

where $N_i = \sum_\sigma X_i^{D\sigma, D\sigma} + 2 X_i^{\psi, \psi}$ and $n_k = \sum_\sigma X_k^{f\sigma, f\sigma}$. The second sum in $\Delta\tilde{H}$ describes density-density interactions between impurity and host lattice sites. The first sum in $\Delta\tilde{H}$ and $\tilde{H}_{sx}$ contain double hopping processes between bands and they are of second order in effective hopping parameters. The effective superexchange integrals are

$$J_{ij}^{DD} = -2A (t_{ij}^{\psi D})^2 > 0, \tag{35}$$

$$J_{ik}^{Db} = -2B (t_{ik}^{\psi b})^2 < 0. \tag{36}$$

By taking the conventional values of the model parameters, $\Delta_{pd} = 4$ eV, $t_{pd} = 1.5$ eV, $t_{pp} = 0.6$ eV, we obtain for the energy differences in the coefficients (24) the following values (in eV):

$$E_\psi - 2E_D \simeq 3.75, \quad E_D + \epsilon_p^{(-)} - E_\psi \simeq 1.09, \quad \epsilon_p^{(-)} - E_D \simeq 4.84.$$

The corresponding hopping parameters and the exchange energies are presented in the Table 2.

The effective energies in (31) are

$$\tilde{E}_D(i) = E_D - \mu + C \sum_{k \neq i} (t_{ik}^{Db})^2, \quad \tilde{\epsilon}_p^{(-)}(k) = \epsilon_p^{(-)} - \mu - C \sum_{i \neq k} (t_{ik}^{Db})^2. \tag{37}$$

15

Values (in eV) of the hopping parameters (17) and the superexchange integrals (35),(36) for the model parameters:

$\Delta_{pd} = 4$ eV, $t_{pd} = 1.5$ eV, $t_{pp} = 0.6$ eV.

R(i-j)	$t_{ij}^{\psi\psi}$	t_{ij}^{DD}	$t_{ij}^{\psi D}$	$t_{ij}^{\psi b}$	t_{ij}^{Db}	J_{ij}^{DD}	J_{ij}^{Db}
$\hat{x}$	0.402	0.454	-0.481	0.384	-0.528	0.124	-0.270
$\hat{x}+\hat{y}$	-0.059	0.022	0.002	-0.095	0.015	$1.6 \cdot 10^{-6}$	-0.017

$$\tilde{E}_\psi(i) = E_\psi - 2\mu + \sum_{j \neq i} J_{ij}^{DD} + \sum_{k \neq i} J_{ik}^{Db}. \tag{38}$$

The shifts of the on-site energies in these equations are of the order of small exchange energies and can be disregarded.

Depending on the position of the chemical potential μ in the one-hole d-like band (electron doping) or the two-hole singlet band (hole doping) one can consider in the low-energy limit only the one-band effective t-J model with the corresponding single site energy in Eq.(31) and the hopping energy in Eq.(32), and the exchange interaction, Eq.(33), which includes both the Cu-Cu and Cu-Zn lattice cell spin exchange interactions. However, the filling of the bands will occur in such a way that after filling the d-like band at first the two-hole singlet band will be filled and only after that the oxygen doublet states at Zn cells can be filled by holes. That becomes evident from comparing the singlet excitation energy $E_\psi - 2E_D \simeq 3.75$ eV and the doublet excitation energy $\epsilon_p^{(-)} - E_D \simeq 4.84$ eV when all Cu cells are occupied by exactly one hole and the Zn cells are empty. So we can understand the spin operator Eq.(29) for the oxygen orbital $|b\sigma>$ at the Zn cell in Eq.(33) as a virtual spin. Exchange interaction of the Cu spin with it just takes into account the second order perturbation due to the hybridisation between singlet states at Cu cells with the oxygen doublet states in the nearest Zn cells. As the estimations show,

we have quite a large ferromagnetic effective exchange interaction between the Cu spin and the virtual oxygen spin at the Zn cell.

5 Conclusions

In the present paper we proposed the effective two-band (p-d) Hubbard model for CuO_2 plane with Zn-impurities, Eq.(18). Based on the band-structure calculations for the model systems, $CaCuO_2$ and Ca_2CuZnO_4, we describe the Zn-impurity as a vacant lattice site in the copper sublattice of $3d$ states while keeping the oxygen sublattice unaffected by Zn substitution. Therefore, in the model the Zn-impurities are not inert substitutions for Cu but show up as oxygen Wannièr states in Zn cells. For the undoped case the excitation energy for the Wannièr states is rather large ($\epsilon_p^{(-)} - E_D \simeq 4.8$ eV) to produce strong effects. However, at finite doping an exchange between holes in the the Cu singlet band and the oxygen Wannièr states at Zn cells can result in a strong scattering due to much smaller excitation energy $E_D + \epsilon_p^{(-)} - E_\psi \simeq 1.1$ eV. This can explain a much stronger reduction of the Néel temperature by Zn impurities at finite doping [4] and finite density of states at the Fermi level in the singlet band [10]-[13]. To study magnetic properties within the model one can use also the effective one-band t-J model, Eq.(30) obtained by further reduction of the two-band model (18). In the t-J model the Zn-impurity cells are described by virtual oxygen spins-1/2 with strong ferromagnetic superexchange interaction (36) with the nearest neighbour Cu sites. By using these microscopical models it is possible to study an influence of Zn impurities both on the antiferromagnetic spin correlations in CuO_2 plane and on the superconducting transition. The results of these studies will be considered elsewhere.

Appendix

The three site part (27) of the effective t-J model can be written in the form:

$$\tilde{H}_{3x} = \sum_{\alpha \in \{A,B,C\}} \alpha \cdot \tilde{H}_{3x}(\alpha), \quad \tilde{H}_{3x}(\alpha) = \tilde{H}_{3x}^{0\psi}(\alpha) + \tilde{H}_{3x}^{DD}(\alpha) + \tilde{H}_{3x}^{S\bar{S}}(\alpha), \quad (A1)$$

where

$$\tilde{H}_{3X}^{0\psi}(A) = \sum_{i \neq j \neq m, \sigma} \{[-\sigma t_{ij}^{\psi D}(t_{jm}^{DD} X_i^{D\sigma,0} X_m^{D\sigma,0} X_j^{0,\psi} + t_{jm}^{\psi\psi} X_j^{\psi,0} X_i^{D\bar{\sigma},\psi} X_m^{D\sigma,\psi}) + \text{H.c.}]$$
$$+ t_{ij}^{\psi D} t_{jm}^{\psi D}(X_j^{\psi,0} X_i^{D\bar{\sigma},\psi} X_m^{0,D\bar{\sigma}} + X_i^{D\sigma,0} X_m^{\psi,D\sigma} X_j^{0,\psi})\}$$
$$+ \frac{1}{2} \sum_{i \neq j \neq k, \sigma} [(t_{ij}^{\psi D} t_{jk}^{\psi b} X_j^{\psi,0} X_i^{D\bar{\sigma},\psi} X_k^{0,b\sigma} - \sigma t_{ij}^{\psi D} t_{jk}^{Db} X_i^{D\sigma,0} X_k^{b\sigma,0} X_j^{0,\psi}$$
$$+ \sigma t_{jk}^{Db} t_{ij}^{\psi D} X_k^{b\sigma,0} X_j^{0,0} X_i^{D\bar{\sigma},\psi} + \sigma t_{jk}^{Db} t_{ij}^{\psi D} X_k^{b\sigma,0} X_j^{D\sigma,D\sigma} X_i^{D\bar{\sigma},\psi}) + \text{H.c.}], \quad (A2)$$

$$\tilde{H}_{3X}^{DD}(A) = \sum_{i \neq j \neq m, \sigma} \{[\sigma t_{ij}^{\psi D}(-t_{jm}^{DD} X_m^{D\sigma,0}(X_j^{0,0} + X_j^{D\sigma,D\sigma}) X_i^{D\bar{\sigma},\psi}$$

$$+ t_{jm}^{\psi\psi} X_i^{D\sigma,0}(X_j^{D\bar{\sigma},D\bar{\sigma}} + X_j^{\psi,\psi}) X_m^{D\bar{\sigma},\psi}) + \text{H.c}] + t_{ij}^{\psi D} t_{jm}^{\psi D}(X_i^{D\sigma,0} X_j^{D\bar{\sigma},D\bar{\sigma}} X_m^{0,D\sigma}$$
$$+ X_i^{D\sigma,0} X_j^{\psi\psi} X_m^{0,D\sigma} - X_m^{\psi,D\sigma} X_j^{0,0} X_i^{D\bar{\sigma},\psi} - X_m^{\psi,D\sigma} X_j^{D\sigma,D\sigma} X_i^{D\bar{\sigma},\psi})\}$$
$$+ \frac{1}{2} \sum_{i \neq j \neq k, \sigma} [t_{ij}^{\psi D} t_{jk}^{\psi b}(X_i^{D\sigma,0} X_j^{D\bar{\sigma},D\bar{\sigma}} X_k^{0,b\sigma} + X_i^{D\sigma,0} X_j^{\psi,\psi} X_k^{0,b\sigma})$$
$$+ \sigma t_{ij}^{\psi D} t_{jk}^{Db}(X_k^{b\sigma,0} X_j^{0,0} X_i^{D\bar{\sigma},\psi} + X_k^{b\sigma,0} X_j^{D\sigma,D\sigma} X_i^{D\bar{\sigma},\psi}) + \text{H.c.}], \quad (A3)$$

$$\tilde{H}_{3x}^{S\bar{S}}(A) = \sum_{i \neq j \neq m, \sigma} \{[\sigma t_{ij}^{\psi D}(-t_{mj}^{DD} X_m^{D\bar{\sigma},0} X_j^{D\sigma,D\sigma} X_i^{D\bar{\sigma},\psi} + t_{jm}^{\psi\psi} X_i^{D\sigma,0} X_j^{D\bar{\sigma},D\sigma} X_m^{D\sigma,\psi}) +$$
$$\text{H.c.}] - X_m^{\psi,D\sigma} X_j^{D\sigma,D\bar{\sigma}} X_i^{D\bar{\sigma},\psi})\}$$
$$- \frac{1}{2} \sum_{i \neq j \neq k, \sigma} [(t_{ij}^{\psi D} t_{jk}^{\psi b} X_i^{D\sigma,0} X_j^{D\bar{\sigma},D\sigma} X_k^{0,b\sigma} + \sigma t_{ij}^{\psi D} t_{jk}^{Db} X_k^{b\sigma,0} X_j^{D\sigma,D\bar{\sigma}} X_i^{D\bar{\sigma},\psi}) + \text{H.c.}], \quad (A4)$$

$$\tilde{H}_{3x}^{0\psi}(B) = [\sum_{i \neq j \neq k, \sigma} \left(\sigma t_{ik}^{\psi b} t_{ij}^{DD} X_j^{D\bar{\sigma},0} X_k^{b\sigma,0} X_i^{0,\psi} - \frac{1}{2} t_{ij}^{\psi D} t_{jk}^{\psi b} X_j^{\psi,0} X_k^{0,b\sigma} X_i^{D\bar{\sigma},\psi}\right)$$
$$- \frac{1}{2} \sum_{i \neq k \neq K, \sigma} \sigma t_{ik}^{\psi b} t_{iK}^{Db} X_k^{b\sigma,0} X_K^{b\bar{\sigma},0} X_i^{0,\psi}] + \text{H.c.}, \quad (A5)$$

$$\tilde{H}_{3x}^{DD}(B) = \sum_{i \neq j \neq k, \sigma} \{[\left(\sigma t_{ik}^{\psi b} t_{ij}^{\psi\psi}(X_k^{b\sigma,0} X_i^{D\bar{\sigma},D\bar{\sigma}} X_j^{D\bar{\sigma},\psi} + X_k^{b\sigma,0} X_i^{\psi,\psi} X_j^{D\bar{\sigma},\psi})$$
$$+ \frac{1}{2}\sigma t_{ik}^{\psi b} t_{jk}^{Db}(X_j^{D\sigma,0} X_k^{0,0} X_i^{D\bar{\sigma},\psi} - X_j^{D\sigma,0} X_k^{b\sigma,b\sigma} X_i^{D\bar{\sigma},\psi}) + \frac{1}{2} t_{ij}^{\psi D} t_{jk}^{\psi b}(X_i^{D\sigma,0} X_j^{D\bar{\sigma},D\bar{\sigma}} X_k^{0,b\sigma}$$
$$+ X_i^{D\sigma,0} X_j^{\psi,\psi} X_k^{0,b\sigma})\right) + \text{H.c.}] + t_{ik}^{\psi b} t_{jk}^{\psi b}(X_j^{\psi,D\sigma} X_k^{0,0} X_i^{D\bar{\sigma},\psi} + X_j^{\psi,D\bar{\sigma}} X_k^{b\sigma,b\sigma} X_i^{D\bar{\sigma},\psi})\}$$
$$+ \sum_{i \neq k \neq K, \sigma} t_{ik}^{\psi b} t_{iK}^{\psi b}(X_k^{b\sigma,0} X_i^{D\bar{\sigma},D\bar{\sigma}} X_K^{0,b\sigma} + X_k^{b\sigma,0} X_i^{\psi,\psi} X_K^{0,b\sigma}) \quad (A6)$$

$$\tilde{H}_{3x}^{S\bar{S}}(B) = \sum_{i \neq j \neq k, \sigma} \{[(\sigma t_{ik}^{\psi b} t_{ij}^{\psi\psi} X_k^{b\sigma,0} X_i^{D\bar{\sigma},D\sigma} X_j^{D\sigma,\psi} - \frac{1}{2}\sigma t_{ik}^{\psi b} t_{jk}^{Db} X_j^{D\sigma,0} X_k^{b\sigma,b\bar{\sigma}} X_i^{D\bar{\sigma},\psi}$$

$$-\frac{1}{2}t_{ij}^{\psi D}t_{jk}^{\psi b}X_i^{D\sigma,0}X_j^{D\bar{\sigma},D\sigma}X_k^{0,b\bar{\sigma}}) + \text{H.c.}] - t_{ik}^{\psi b}t_{jk}^{\psi b}X_j^{\psi,D\sigma}X_k^{b\sigma,b\bar{\sigma}}X_i^{D\bar{\sigma},\psi}\}$$

$$-\sum_{i\neq k\neq K,\sigma} t_{ik}^{\psi b}t_{iK}^{\psi b}X_k^{b\sigma,0}X_i^{D\sigma,D\sigma}X_K^{0,b\bar{\sigma}}, \tag{A7}$$

$$\tilde{H}_{3x}^{0\psi}(C) = \{ \sum_{i\neq j\neq k,\sigma} [-\frac{1}{2}\sigma t_{ij}^{\psi D}t_{jk}^{Db}X_i^{D\sigma,0}X_k^{b\bar{\sigma},0}X_j^{0,\psi} - t_{ik}^{Db}t_{ij}^{\psi\psi}X_j^{D\sigma,\psi}X_k^{0,b\sigma}X_i^{\psi,0}]$$

$$-\frac{1}{2}\sum_{i\neq k\neq K,\sigma} \sigma t_{ik}^{\psi b}t_{iK}^{Db}X_k^{b\sigma,0}X_K^{b\bar{\sigma},0}X_i^{0,\psi}\} + \text{H.c.}, \tag{A8}$$

$$\tilde{H}_{3x}^{DD}(C) = \sum_{i\neq j\neq k,\sigma} \{[\left(t_{ik}^{Db}t_{ij}^{DD}(X_j^{D\sigma,0}X_i^{0,0}X_k^{0,b\sigma} + X_j^{D\sigma,0}X_i^{D\sigma,D\sigma}X_k^{0,b\bar{\sigma}})\right.$$

$$-\frac{1}{2}\sigma t_{ij}^{\psi D}t_{jk}^{Db}(X_k^{b\sigma,0}X_j^{0,0}X_i^{D\bar{\sigma},\psi}+X_k^{b\sigma,0}X_j^{D\sigma,D\sigma}X_i^{D\bar{\sigma},\psi})+\frac{1}{2}\sigma t_{ik}^{\psi b}t_{jk}^{Db}(X_j^{D\sigma,0}X_k^{b,0}X_i^{D\bar{\sigma},\psi}$$

$$\left.+X_j^{D\sigma,0}X_k^{b\sigma,b\sigma}X_i^{D\bar{\sigma},\psi})\right) + \text{H.c.}] + t_{ik}^{Db}t_{jk}^{Db}(X_i^{D\sigma,0}X_k^{0,0}X_j^{0,D\sigma} + X_i^{D\sigma,0}X_k^{b\sigma,b\sigma}X_j^{0,D\sigma})\}$$

$$-\sum_{i\neq k\neq K,\sigma} t_{ik}^{Db}t_{iK}^{Db}(X_K^{b\sigma,0}X_i^{0,0}X_k^{0,b\sigma} + X_K^{b\sigma,0}X_i^{D\sigma,D\sigma}X_k^{0,b\sigma}), \tag{A9}$$

$$\tilde{H}_{3x}^{S\bar{S}}(C) = \sum_{i\neq j\neq k,\sigma} \{[(t_{ik}^{Db}t_{ij}^{DD}X_j^{D\bar{\sigma},0}X_i^{D\sigma,D\bar{\sigma}}X_k^{0,b\sigma} - \frac{1}{2}\sigma t_{jk}^{Db}t_{ij}^{\psi D}X_k^{b\bar{\sigma},0}X_j^{D\sigma,D\bar{\sigma}}X_i^{D\bar{\sigma},\psi}$$

$$+\frac{1}{2}\sigma t_{ik}^{\psi b}t_{jk}^{Db}X_j^{D\sigma,0}X_k^{b\sigma,b\bar{\sigma}}X_i^{D\bar{\sigma},\psi}) + \text{H.c.}] + t_{ik}^{Db}t_{jk}^{Db}X_i^{D\sigma,0}X_k^{b\sigma,b\sigma}X_j^{0,D\bar{\sigma}}\}$$

$$-\sum_{i\neq k\neq K,\sigma} t_{ik}^{Db}t_{iK}^{Db}X_K^{b\bar{\sigma},0}X_i^{D\sigma,D\bar{\sigma}}X_k^{0,b\sigma}, \tag{A10}$$

where $i,j,m \ni$ Cu cells and $k,K \ni$ Zn cells and in the summation all three lattice cites are different.

References

[1] N.M. Plakida, *High-Temperature Superconductors* (Springer, Berlin, 1995).

[2] A.V. Narlikar, C.V.N. Rao, and S.K. Agrawal, In: *Studies of High Temperature Superconductors*, edited by A. Narlikar (Nova Science Publishers, New York, 1989) Vol. 1, p. 341.

[3] G. Xiao, M.Z. Cieplak and C.L. Chien, Phys. Rev. B **42** 240 (1990)

[4] H. Alloul, P. Mendels, H. Casalta, J.F. Marucco, and J. Arabski, Phys. Rev. Lett. **67**, 3140 (1991).

[5] G. Xiao, M.Z. Cieplak, J.Q. Xiao and C.L. Chien, Phys.Rev. B **42**, 8752 (1990).

[6] A.V. Mahajan, H. Alloul, G. Collin and J.F. Marucco, Phys. Rev. Lett. **72**, 3100 (1994).

[7] A.M. Finkelstein, V.E. Kataev, E.F. Kukovitskii, and G.B. Teitel'baum, Physica C **168**, 370 (1990).

[8] P. Mendels, H. Alloul, J.H. Brewer, G.D. Morris, T.L. Duty, E.J. Ansaldo, G. Collin, J.F. Marucco, C. Niedermayer, D.R. Noakes, and C.E. Stronach, Phys. Rev. B **49**, 10035 (1994).

[9] K. Ishida, Y. Kitaoka, K. Yamozoe, and K. Asayama, Phys. Rev. Lett. **76**, 531 (1996).

[10] K. Ishida, Y. Kitaoka, T. Yoshitomi, N. Ogata, T. Kamino, and K. Asayama, Physica C **179** (1991) 29-38; K. Ishida, Y. Kitaoka,

T. Yoshitomi, N. Ogata, T. Kamino and K. Asayama, J.R. Cooper, and N. Athanassopoulou, J. Phys. Soc. Jpn. **62**, 2803 (1993).

[11] A. Jánossy, J.R. Cooper, L.-C. Brunel, A. Carrington, Phys. Rev. B **50**, 3442 (1994).

[12] G.V.M. Williams, J.L. Tallon, R. Meinhol, A. Jánossy, Phys. Rev. B **51**, 16 503 (1995).

[13] J.W. Loram, K.A. Mirza and P.F. Freeman, Physica C **171** (1990) 243-256.

[14] K. Kakurai, S. Shamoto, T. Kiyokura, M. Sato, J.M. Tranquada, and G. Shirane, Phys. Rev. B **48**, 3485 (1993).

[15] Y. Sidis, P. Bourges, B. Hennion, L.P. Regnault, R. Villeneuve, G. Collin, J.F. Marucco, Phys. Rev. B **53**, 6811 (1996).

[16] T.R. Chien, Z.Z. Wang, and N.P. Ong, Phys. Rev. Lett. **67**, 2088 (1991).

[17] D.J. Walker, A.P. Mackenzie and J.R. Cooper, Phys. Rev. B **51**, 15 653 (1995).

[18] Y. Fukuzumi, K. Mizuhashi, K. Takenaka, and S. Uchida, Phys. Rev. Lett. **76**, 684 (1996).

[19] R.E. Walstedt, R.F. Bell, L.F. Schneemeyer, J.V. Waszczak, W.W. Warren, Jr., R. Dupree, and A. Gencten, Phys. Rev. B **48**, 10 646 (1993).

[20] P. Fulde and G. Zwicknagl, in *Earlier and Recent Aspects of Superconductivity*, eds. J.G. Bednorz, K.A. Müller, (Springer-Verlag, Berlin, Heidelberg, 1990), p. 326.

[21] P. Sen, S. Basu, and A. Singh, Phys. Rev. B **50**, 10 381 (1994).

[22] W. Ziegler, D. Poilblanc, R. Preuss, W. Hanke, and D.J. Scalapino, Phys. Rev. B **53**, 8704 (1996).

[23] D. Poilblanc, D.J. Scalapino, and W. Hanke, Phys. Rev. Lett. **72**, 884 (1994).

[24] S.A. Krivenko, G.G. Khaliullin, JETP Lett. **62**, 723 (1995); Physica C **244**, 83 (1995).

[25] G.K. Khaliullin, R. Kilian, S. Krivenko and P. Fulde, Phys. Rev. B **56**, 11882 (1997); Physica C **282-287**, 1749 (1997).

[26] N. Nagaosa, T.-K. Ng, J. Phys. Chem. Solids **56**, 1737 (1995); Phys. Rev. B **51** 15588 (1995).

[27] B.C. Hertog, M.P. Das, Physica C **282-287**, 1709 (1997).

[28] T. Hotta, J. Phys. Soc. Jpn. **62**, 274 (1993).

[29] P.J. Hirschfeld and N. Goldenfeld, Phys. Rev. B **48**, 4219 (1993).

[30] D.S. Hirashima, Phys. Rev. B **50**, 10 142 (1994).

[31] P. Montoux and D. Pines, Phys. Rev. B **49**, 4261 (1994).

[32] D. Pines, Physica C **235-240**, 113 (1994).

[33] V.J. Emery, Phys. Rev. Lett. **58**, 2794 (1987).

[34] C.M. Varma, S. Schmitt-Rink, E. Abrahams, Solid State Commun. **62**, 681 (1987)

[35] S.V. Lovtsov, and V.Yu. Yushankhai, Physica C **179**, 159 (1991).

[36] J.H. Jefferson, H. Eskes, and L.F. Feiner, Phys. Rev. B **45**, 7959 (1992).

[37] V.I. Belinicher and A.L. Chernyshev, Phys. Rev. B **49**, 9746 (1994).

[38] N.M.Plakida, R.Hayn, and J.-L. Richard, Phys. Rev. B **51**, 16 599 (1995).

[39] V.Yu. Yushankai, V.S. Oudovenko, R. Hayn, Phys. Rev. B **55**, 15 562 (1997).

[40] F.C. Zhang and T.M. Rice, Phys. Rev. B **37**, 3759 (1988).

[41] L.F. Mattheiss and D.R. Hamann, Phys. Rev. B **40**, 2217 (1989).

[42] H. Eschrig, *Optimized LCAO Method*, 1. ed. (Springer, Berlin, 1989).

[43] B.S. Shastry, Phys. Rev. Lett. **63**, 1288 (1989).

[44] R. Raimondi, J.H. Jefferson, and L.F. Feiner, Phys. Rev. B **53**, 8774 (1996).

[45] J.R. Schrieffer, P.A. Wolff, Phys. Rev. **149**, 491 (1966).

24

Ковачевич Ж., Хайн Р., Плакида Н.М.   E17-98-324
Эффективная модель Хаббарда для плоскости CuO$_2$
с примесями Zn

В рамках кластерной теории возмущений на основе p–d модели построена двухзонная модель Хаббарда для медно-оксидной плоскости с малой концентрацией примесей Zn. Примесные состояния Zn на вакантных Cu-узлах описаны одночастичными кислородными состояниями Ванье. Предлагаемая модель основана на результатах расчетов зонной структуры, полученных в рамках приближения локальной плотности. Последующая редукция двухзонной модели к однозонной t–J модели указывает на существование ферромагнитного сверхобменного взаимодействия между Cu-спинами и ближайшими спинами в Zn-ячейках.

Работа выполнена в Лаборатории теоретической физики им. Н.Н.Боголюбова ОИЯИ.

Kovačević Ž., Hayn R., Plakida N.M.   E17-98-324
Effective Hubbard Model for Zn-Doped CuO$_2$ Plane

In the framework of the cell-perturbation method for the original p–d model an effective two-band Hubbard model for the CuO$_2$ plane with Zn impurities is derived. Zn impurities are modelled by Wannièr oxygen one-hole states at vacant Cu sites. The model is based on the results of band structure calculations carried out within the local-density approximation. Further reduction to an extended t–J model shows a large ferromagnetic superexchange interaction between the Cu spin with the nearest virtual oxygen spin in the Zn cell.

The investigation has been performed at the Bogoliubov Laboratory of Theoretical Physics, JINR.